

## Probabilistic Fragility Analysis for Seismic Liquefaction of Sites

Jian-Yu Meng<sup>1</sup> and Da-Gang Lu<sup>2</sup>

<sup>1</sup>School of Civil Engineering, Harbin Institute of Technology, Harbin, China.  
E-mail: 20b933028@stu.hit.edu.cn

<sup>2</sup>School of Civil Engineering, Harbin Institute of Technology, Harbin, China.  
E-mail: ludagang@hit.edu.cn

**Abstract:** Seismic liquefaction is a very complex and uncertain problem, which is affected by many factors such as earthquake intensity, site conditions, soil properties, etc. During the past half a century, the state-of-the-art in analysis and evaluation of earthquake-induced soil liquefaction and its consequences as well as the state-of-the-practice in improving seismic stability to resist liquefaction have been made much progress. However, the fragility analysis and assessment for seismic liquefaction of sites have not been paid enough attentions to. In this paper, the concept of seismic liquefaction fragility for building sites is proposed. The soil resistance to liquefaction and liquefaction possibility are expressed as a fragility function of ground motion intensity, which can be used to describe minor, medium and severe liquefaction potential under different ground motion intensity. Combined with the existing research results of seismic liquefaction evaluation, the analysis method of liquefaction fragility is given. Taking a specific site as an example for liquefaction fragility analysis, it is found that taking the calculated exceedance probability of different liquefaction levels as the observation value, the liquefaction fragility function follows lognormal distribution. With the increase of liquefaction level, the median value of liquefaction fragility function increases, while the site liquefaction fragility curve moves to the right, which shows that the ability of the site to resist more severe liquefaction is increasing. When convolved with the analysis results of liquefaction triggering and hazard, the liquefaction fragility function can be a much efficient tool for seismic liquefaction risk analysis of specific sites.

Keywords: seismic liquefaction; liquefaction fragility; liquefaction probability; liquefaction potential

### 1 Introduction

Earthquake-induced soil liquefaction is a main cause of earthquake damage worldwide, which causes great damage to underground structure facilities, and directly lead to the loss of foundation bearing capacity and damage to ground buildings. In the 1995 Kobe earthquake in Japan, liquefaction of natural soil layer and artificial soil filling occurred in a large range along the coastline, which caused serious damage to ground and underground structures (Elgamalet al. 1996; Hatanaka et al. 1997). Liquefaction was widely distributed during the 2008 Wenchuan earthquake. In this earthquake, liquefaction of deep soil and gravel occurred in many areas, resulting in sand blasting and water blasting that damaged large areas of farmland crops. The 2011 New Zealand earthquake caused severe damage to a large number of surface structures and underground facilities, most of which were caused by site liquefaction and lateral movement, and even repeated liquefaction. In 2016, the Meinong Earthquake in Taiwan caused a soil liquefaction crisis in Taiwan, and the liquefaction damage far exceeded the earthquake damage level.

In the past few decades, a large amount of data and research results have been accumulated on earthquake-induced soil liquefaction. Estimating liquefaction triggering is the primary problem. An empirical stress-based approach for liquefaction triggering assessment called the "simplified method" which is first developed by Seed (1971) is the most commonly used in practice. Based on the "simplified method", many scholars modified the calculation formula considering the impact of earthquake magnitude, overburden pressure, clay content and other factors (Seed 1982; Boulanger and Idriss 2012). The evaluations of liquefaction resistance and liquefaction potential of the sites are mainly based on four in-situ tests (Andrus and Kenneth 2000; Howie and Vaid 2000; Cao et al. 2013), including the standard penetration, cone penetration, dynamic cone penetration or Becker penetration, and wave velocity tests. Besides, some scholars have developed new analytical techniques, screening tools, and models to assess liquefaction triggering and post-liquefaction consequences, using artificial neural network, logistic regression, Bayesian network and other methods (Huang et al. 2012).

In this paper, an analytical approach that incorporates the site conditions and seismicity to evaluate the liquefaction of a site is introduced. By using this analytical method, a probabilistic method for evaluating liquefaction potential for earthquakes with a given ground motion intensity is presented and illustrated. Then the earthquake-induced liquefaction potential probability matrix and the fragility curves are constructed. The soil resistance to liquefaction and liquefaction possibility are expressed as a fragility function of ground motion intensity, which can be used to quantitatively describe the severity of liquefaction under different ground motion intensities.

## 2 Concept and model of seismic liquefaction fragility for sites

### 2.1 Concept of site seismic liquefaction fragility

Earthquake-induced soil liquefaction is affected by the site condition (Idriss and Boulanger 2008), such as relative density, percentage of clay content, and effective confining pressure, which is unable to probe below the surface completely and have strong spatial variability. In addition, it is also affected by seismic parameters such as earthquake intensity, frequency content, and duration of an earthquake. The probabilistic description of liquefaction or anti-liquefaction capacity of the site for an earthquake with a given ground motion intensity is still insufficient. Therefore, it is necessary to consider the randomness of the site conditions and ground motions, building the probability relationship between site liquefaction level and earthquake intensity, to express the soil resistance to liquefaction and liquefaction possibility under different ground motions. The seismic liquefaction fragility for site is defined as the probability that the component reaches or exceeds liquefaction state of interest, given a particular ground motion intensity:

$$F_R(x) = P[LS | IM = x] \quad (1)$$

where  $F_R()$  is the liquefaction fragility which is the probability of being a to exceed a particular damage state,  $LS$ , for a given seismic intensity level defined by the earthquake parameter,  $IM$ .

### 2.2 Function of seismic liquefaction fragility of site

The seismic liquefaction fragility function represents the probability distribution of site liquefaction level for an earthquake with a given ground motion intensity. A lognormal cumulative distribution function is often used to define a fragility function:

$$F_R(LS | IM = x) = \Phi\left(\frac{\ln(x/\theta)}{\beta}\right) \quad (2)$$

where  $\Phi()$  is the standard cumulative probability function,  $\theta$  denotes the median value of the distribution, and  $\beta$  denotes the logarithmic standard deviation.

An appropriate estimation procedure is needed and then used to estimate fragility functions. The maximum likelihood method is carried out. The transcendence probabilities of different liquefaction levels are taken as observation values. The optimal solution of the parameters of fragility functions is found by solving the minimum sum of squared errors between the observed values and the predicted values by the fragility function. Mathematically, this is stated as follows (see Baker (2015)):

$$\{\hat{\theta}, \hat{\beta}\} = \underset{\theta, \beta}{\operatorname{argmin}} \sum_{j=1}^m \left[ \frac{z_j}{n_j} - \Phi\left(\frac{\ln(x_j/\theta)}{\beta}\right) \right]^2 \quad (3)$$

where  $m$  is the number of  $IM$  levels,  $z_j$  is the number of different liquefaction levels with  $IM=x_j$ ,  $n_j$  is the number of  $IM=x_j$ .

### 2.3 Site liquefaction level and liquefaction seismic fragility

According to Iwasaki's research, the earthquake-induced liquefaction levels of the site have been divided into four levels: basically non-liquefaction ( $DS_0$ ), minor liquefaction ( $DS_1$ ), moderate liquefaction ( $DS_2$ ) and severe liquefaction ( $DS_3$ ). Earthquake is the direct cause of site liquefaction, which itself has great randomness. The probability of site being in a certain liquefaction state is the conditional probability of earthquake with a specific ground motion intensity:

$$P_{DS_i}(x) = P[DS_i | IM = x] \quad (4)$$

where  $P_{DS_i}(x)$  is the probability of a specific liquefaction level  $DS_i$  with  $IM=x$ .

The seismic liquefaction fragility of the site is defined as the conditional probability of the site reaching or exceeding the corresponding liquefaction level under an earthquake with a given intensity. The liquefaction fragility curve is used to describe the transcendental probability of the site corresponding to different liquefaction levels under different ground motions. The fragility is calculated as follows:

$$\begin{cases} F_{R_1}(x) = 1 - P_{DS_0}(x) \\ F_{R_2}(x) = P_{DS_2}(x) + P_{DS_3}(x) \\ F_{R_3}(x) = P_{DS_3}(x) \end{cases} \quad (5)$$

where all variables are as defined earlier.

### 3 Evaluation procedure for seismic liquefaction fragility of site

#### 3.1 Calculation of anti-liquefaction safety factor

The safety factors in engineering seismic codes are similar in different countries. Concretely, the factor of safety against liquefaction is defined in terms of *CSR*(cyclic stress ratio), *CRR*(cyclic resistance ratio), and *MSF*(magnitude scaling factor):

$$F_L = \left( \frac{CRR_{7.5}}{CSR} \right) \cdot MSF \quad (6)$$

where  $F_L$  is the safety factor of anti-liquefaction and  $CRR_{7.5}$  is soil liquefaction resistance of saturated pure sand with  $M_w = 7.5$ .

The equivalent cyclic stress ratio is calculated using 65% of the peak cyclic stress under earthquake action as the representative value:

$$CSR = 0.65 \frac{\tau_{\max}}{\sigma'_0} \quad (7)$$

where  $\tau_{\max}$  is peak cyclic stress and  $\sigma'_0$  is effective vertical overburden pressure.

The cyclic resistance ratio is calculated according to the formula given by Youd and Idriss (2001), which is applicable to the calculation of the clean sand:

$$CRR_{7.5} = \frac{1}{34 - (N_1)_{60}} + \frac{(N_1)_{60}}{135} + \frac{50}{[10 \cdot (N_1)_{60} + 45]^2} - \frac{1}{200} \quad (8)$$

*MSF* is calculated according to the formula given by Youd and Idriss (2001):

$$MSF = 10^{2.24} / M_w^{2.56} \quad (9)$$

#### 3.2 Calculation of liquefaction potential index

The liquefaction potential index (LPI) is calculated and evaluated using the method proposed by Iwasaki (1984):

$$LPI = \int_0^{20} F(z)W(z)dz \quad (10)$$

$$F(z) = \begin{cases} 1 - F_L & (F_L \leq 1.0) \\ 0 & (F_L > 1.0) \end{cases} \quad (11)$$

$$W(z) = \begin{cases} 10 - 0.5z & (z < 20\text{m}) \\ 0 & (z > 20\text{m}) \end{cases} \quad (12)$$

where  $z$  is the depth of a point in the soil layer from the surface.

The classification criteria of liquefaction severity is shown in Table 1.

**Table 1.** Liquefaction severity classification criteria

Criteria	Liquefaction classification
LPI=0	Basically non-liquefaction
$0 < LPI \leq 5$	Minor liquefaction
$5 < LPI \leq 15$	Moderate liquefaction
$LPI > 15$	Severe liquefaction

### 3.3 Evaluation procedure of site seismic liquefaction fragility

The seismic liquefaction fragility for sites reflects the uncertainty transmission from ground motion intensity parameters to the site conditions by establishing the probabilistic relationship between site liquefaction level and ground motion intensity. The assessment process of seismic liquefaction fragility for site is shown in Figure 1.

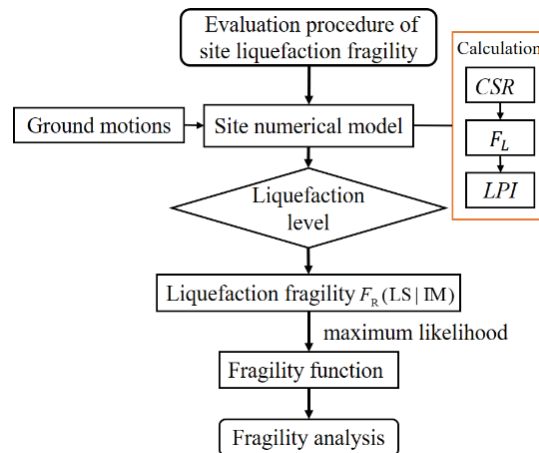


Figure 1. Evaluation procedure of site seismic liquefaction fragility

## 4 Case study

### 4.1 Site conditions and numerical model

In the study of site earthquake-induced liquefaction, assessment of initiation of soil liquefaction in the site is carried out firstly. It mainly distinguishes whether soil layers are liquefiable, then the soil layers which is likely to be liquefied will be given a further identification. This work mainly discusses the liquefaction of sand layer in the site. The parameters of soil material constitutive model have been set according to Khosravifar et al. (2018). The stratification and properties of layer 6 in the site are determined by the borehole bar chart of an engineering geology in Xi'an area, the shear wave velocity test results and the soil dynamic laboratory test results, and see Tables 2 and 3 for soil dynamic property parameters.

Table 2. Soil dynamic property parameters within 20m below the surface

Layer number	Soil type	Layer thickness (m)	$(N_1)_{60}$	$D_r$ (%)	Clean sand (Y or N)
1	Loose sand	4	5	33	Y
2	Medium clay	4	-	-	-
3	Loose sand	5	5	33	Y
4	Medium dense sand	4	15	57	Y
5	Dense sand	3	25	74	Y

Table 3. Soil dynamic property within a depth of more than 20m

Layer number	Shear modulus ratio		Shear strain ( $10^{-4}$ )							
	Damping ratio		0.05	0.1	0.5	1.0	5.0	10.0	50.0	100.0
6	Shear modulus ratio		0.9959	0.9908	0.952	0.9075	0.6607	0.4931	0.1628	0.0886
	Damping ratio		0.0112	0.0135	0.0222	0.0311	0.0612	0.0753	0.0977	0.1021

This calculation uses OpenSees for modeling and analysis. As mentioned above, the liquefaction potential calculation mainly considers the liquefaction potential of soil within 20m below the surface. For soil properties with a depth of more than 20m, the specified shear modulus attenuation curve is used to define the yield surface. See the table for specific parameters, and the PIMY material model is used. Within 20m below the surface, there are mainly sandy soil and clay. The sandy soil adopts the PDMY03 material model (Qiu and Elgamel 2020), the clay adopts the PIMY material model. The soil parameters are calibrated by Khosravifar et al. (2018).

Considering the calculation efficiency and accuracy, a two-dimensional soil column model with cell size no more than 1m has been established. Since site liquefaction is a complex dynamic reaction result of soil and water coupling, Therefore, the U-P unit which can take pore water pressure into account has been used for soil modeling. In the seismic response analysis of horizontal free site, the viscous boundary condition is set at the bottom and the velocity time history is input for dynamic analysis.

## 4.2 Ground motions

In this work, the seismic records of rock site(outcrop bedrock) with equivalent shear wave velocity  $V_{s30}$  greater than 500m/s and less than 1500m/s are selected for the analysis. At the same time, the seismic analysis does not consider the influence of near-fault ground motion with special properties. The fault distance of selected ground motion is greater than 10km. In order to avoid the obvious tendency of the results caused by the selection of ground motion, this paper selects the general ground motion records based on the  $M_w$ - $R$  strip. The four ground motion strips are as follows:

SMSR (Small magnitude and small distance),  $5.5 < M_w < 6.7$ ,  $10 < R < 50$ km;

LMSR (Large Magnitude and small distance),  $6.7 < M_w < 8.0$ ,  $10 < R < 50$ km;

SMLR (Small Magnitude and large distance),  $5.5 < M_w < 6.7$ ,  $50 < R < 100$ km;

LMLR (Large Magnitude and large distance),  $6.7 < M_w < 8.0$ ,  $50 < R < 100$ km.

90 seismic events have been selected from the PEER database, including the Northridge earthquake in 1994, Loma Prieta earthquake in 1989, Kobe earthquake in Japan in 1995, Chi-chi earthquake in Taiwan in 1999, etc. The  $M_w$ - $R$  distribution of selected ground motion records is shown in Figure 2.

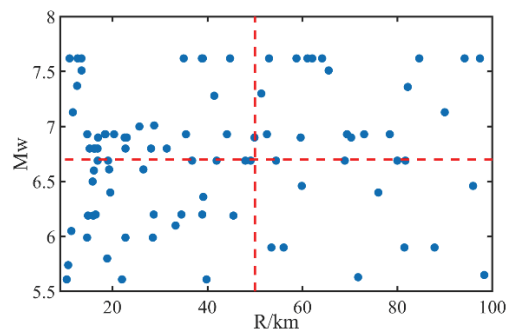


Figure 2.  $M_w$ - $R$  distribution

A total of 180 ground motions in horizontal two directions have been selected from 90 ground motions. The 180 ground motions have been amplitude-modulated for 20 times, with an amplitude modulation range of 0.02g~0.4g and an amplitude modulation interval of 0.02g, respectively, to obtain 3600 ground motions after amplitude-modulated, which are respectively input into the model for calculation.

## 4.3 Fragility curves

After amplitude modulation according to PGA, the seismic liquefaction fragility of the site is calculated according to PGA, PGD, IA and CAV respectively. Considering the number of samples in each index division interval and the correlation between LPI and IMs, PGV is finally selected as the IM, and the author has carried out detailed work in another work. Taking PGV as the ground motion intensity parameter, the calculation results under different liquefaction levels are counted according to the interval of 0.3cm/s. The seismic liquefaction fragility curves under minor, medium and severe liquefaction levels are obtained according to the fragility calculation procedure mentioned above, as shown in Figure 3. The red horizontal dotted line in Figure 3 is the 50% probability boundary.

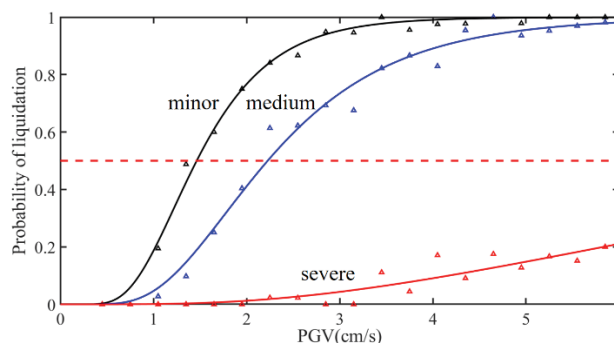


Figure 3. Liquefaction fragility curves for different liquefaction levels

In Figure 4, the fragility curves of severe liquefaction are not fully displayed, because PGV needs to be increased to a certain extent so that the fragility curve of severe liquefaction will exceed the 50% probability boundary. The fragility curve of severe liquefaction is shown in Figure 4 completely.

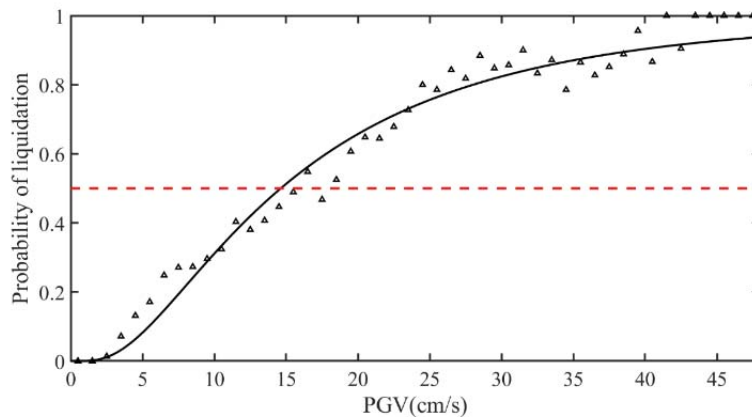


Figure 4. The fragility curve of severe liquefaction

## 5 Conclusions

(1) The liquefaction level of the site is closely related to the ground motion intensity. In this paper, the conditional probability of the liquefaction level under different ground motion intensity has been calculated, and the fragility analysis procedure is introduced to analyze the earthquake-induced liquefaction. The liquefaction fragility can evaluate the liquefaction level and anti-liquefaction ability of the site under different ground motion intensity in the sense of probability.

(2) Taking the calculated exceedance probability of different liquefaction levels as the observation value, it basically conforms to the lognormal distribution. The lognormal distribution can be used as the liquefaction fragility function, and its parameters can be estimated with the help of the maximum likelihood method to further obtain the liquefaction fragility curve.

(3) The liquefaction fragility of the site has been calculated and analyzed. With the improvement of liquefaction level, the median value of liquefaction fragility function increases and the site liquefaction fragility curve moves to the right, which reflects the enhancement of the ability of the site to resist more serious liquefaction.

## Acknowledgments

This work is supported by National Key Research and Development Plan of China (2021YFB2600500). Opinions and findings presented are those of the writers and do not necessarily reflect the views of the sponsors.

## References

- Andrus, R.D., and Kenneth, I.I. (2000). Liquefaction resistance of soils from shear-wave velocity. *Journal of Geotechnical and Geoenvironmental Engineering*, 126(11), 1015-1025.
- Boulanger, R.W., and Idriss, I.M. (2012). Probabilistic standard penetration test-based liquefaction-triggering procedure. *Journal of Geotechnical and Geoenvironmental Engineering*, 138(10), 1185-1195.
- Baker, J.W. (2015). Efficient Analytical Fragility Function Fitting Using Dynamic Structural Analysis. *Earthquake Spectra*, 31(1).
- Cao, Z.Z., Youd, T.L., Yuan, X.M. (2013). Chinese dynamic penetration test for liquefaction evaluation in gravelly soils. *Journal of Geotechnical and Geoenvironmental Engineering*, 139(8).
- Elgamal, A.W., Zeghal, M., and Parra, E. (1996). Liquefaction of reclaimed island in kobe, japan. *Journal of Geotechnical Engineering*, 122(1), 39-49.
- Hatanaka, M., Uchida, A., and Ohara, J. (1997). Liquefaction characteristics of a gravelly fill liquefied during the 1995 hyogo-ken nanbu earthquake. *Journal of the Japanese Geotechnical Society Soils & Foundation*, 37(3), 107-115.
- Howie, J.A., and Vaid, Y.P. (2000). Evaluating cyclic liquefaction potential using the cone penetration test: discussion. *Canadian Geotechnical Journal*, 37(1), 270-271.
- Huang, H.W., Zhang, J., Zhang, L.M. (2012). Bayesian network for characterizing model uncertainty of liquefaction potential evaluation models. *Journal of Civil Engineering, KSCE*.
- Iwasaki, T., Arakawa, T., and Tokida, K. I. (1984). Simplified procedures for assessing soil liquefaction during earthquakes. *International Journal of Soil Dynamics & Earthquake Engineering*, 3(1), 49-58.
- Idriss, I.M., and Boulanger, R.W. (2008). Soil liquefaction during earthquakes. *Earthquake Engineering Research Institute*.
- Khosravifar, A., Elgamal, A., Lu, J., & Li, J. (2018). A 3d model for earthquake-induced liquefaction triggering and post-liquefaction response. *Soil Dynamics and Earthquake Engineering*, 110.



- Qiu, Z., and Elgamal, A. (2020). Numerical simulations of LEAP centrifuge tests for seismic response of liquefiable sloping ground. *Soil Dynamics and Earthquake Engineering*, 139, 106378.
- Seed, H.B. (1971). Simplified procedure for evaluating soil liquefaction potential. *J. of the Soil Mechanics and Foundation Division*, 97.
- Seed, H.B. (1982). Ground Motions and soil liquefaction during earthquakes. *Earthquake Engineering Research Institute*.
- Youd, T.L., and Idriss, I.M. (2001). Liquefaction resistance of soils: summary report from the 1996 NCEER and 1998 NCEER/NSF workshops on evaluation of liquefaction resistance of soils. *Journal of Geotechnical & Geoenvironmental Engineering*, 127(10).